2494–2502 *Nucleic Acids Research, 2000, Vol. 28, No. 13*

Quantitative characterization of the interaction between purified human estrogen receptor α and DNA using fluorescence anisotropy

Mireille Boyer, Nicolas Poujol, Emmanuel Margeat and Catherine A. Royer*

Centre de Biochimie Structurale, 29 rue de Navacelles, 34090 Montpellier cedex, France

Received March 23, 2000; Revised and Accepted May 16, 2000

ABSTRACT

In an effort to better define the molecular mechanisms of the functional specificity of human estrogen receptor α, we have carried out equilibrium binding assays to study the interaction of the receptor with a palindromic estrogen response element derived from the vitellogenin ERE. These assays are based on the observation of the fluorescence anisotropy of a fluorescein moiety covalently bound to the target oligonucleotide. The low anisotropy value due to the fast tumbling of the free oligonucleotide in solution increases substantially upon binding the receptor to the labeled ERE. The quality of our data are sufficient to ascertain that the binding is clearly cooperative in nature, ruling out a simple monomer interaction and implicating a dimerization energetically coupled to DNA binding in the nanomolar range. The salt concentration dependence of the affinity reveals formation of high stoichiometry, low specificity complexes at low salt concentration. Increasing the KCl concentration above 200 mM leads to specific binding of ER dimer. We interpret the lack of temperature dependence of the apparent affinity as indicative of an entropy driven interaction. Finally, binding assays using fluorescent target EREs bearing mutations of each of the base pairs in the palindromic ERE half-site indicate that the energy of interaction between ER and its target is relatively evenly distributed throughout the site.

INTRODUCTION

The estrogen receptor (ER) is a member of the nuclear receptor family of ligand activated transcriptional regulators (1,2). In response to estrogens, this protein activates transcription of a number of genes in mammalian cells including vitellogenin, cathepsin D, transforming growth factor α and the oncogene product *c-fos*. The action of estrogens has been linked to the development of uterine, breast and endometrial cancers. ER shares a strong homology with other members of the nuclear receptor family, those both closely and more distantly related, such as the glucocorticoid receptor and the androgen receptor, or the vitamin D, retinoic acid and retinoid X receptors. These proteins are made up of an N-terminal transactivation domain, a central DNA binding and dimerization domain, and a C-terminal ligand binding, dimerization and transactivation domain in addition to linker regions and determinants for nuclear translocation.

Given the involvement of these proteins in a large number of human pathologies, they have been the target of drug development for some time, and anti-estrogens, for example, are widely used in the treatment of breast cancer. A thorough, quantitative understanding of the structure–energetics–function relations in these systems would greatly contribute to the elaboration of novel therapeutic approaches to the treatment of human pathologies involving the estrogen receptor. A number of quantitative biophysical studies of the interactions between purified full-length ER and its various biological partners have been published. For example, Gorski and co-workers (3–7) examined ER–DNA interactions using pull-down methods. While these studies yielded precise values for the apparent affinities, they were carried out using cell extract, rather than purified receptor, such that extrinsic factors may have participated in the complexation. Their results (3,5) suggested that estradiol binding did not affect ER interaction with its EREs and that the protein bound as a monomer. A certain number of gel retardation studies have also appeared (i.e., 8–12) in which the interactions between ER and DNA, the effects of ligand and target sequence were explored. This method provides interesting information concerning the number of stoichiometric complexes formed, but suffers from its non-equilibrium nature and the relatively low signal-to-noise ratio inherent in the titration curves derived from quantification of the bands. The quality of such data is insufficient for determination of the presence and degree of cooperativity in binding. Recent studies of ER–ERE interactions based on surface plasmon resonance suggest ligand dependence in ER–ERE interactions (13) in contradiction with the earlier work of Gorski and co-workers (3,5). However, mass transport effects, in addition to the overall non-equilibrium nature of these measurements, renders desirable the use of a true equilibrium method for evaluating the affinity and cooperativity of ER–ERE interactions and for testing the effects of salt, ligand binding, temperature and target sequence on these interactions. A series of in-depth thermodynamic studies on glucocorticoid receptor DNA binding domain (GR-DBD) interactions with glucocorticoid and estrogen response elements (GRE and ERE) targets has

*To whom correspondence should be addressed. Tel: +33 4 67 41 79 02; Fax: +33 4 67 41 79 13; Email: royer@tome.cbs.univ-montp1.fr

provided fundamental information concerning the underlying biophysics of these interactions (14,15). However, it is important to address the eventual role of the rest of the nuclear receptor proteins by comparing results obtained with the isolated DNA binding domain to those that can be obtained using the full-length proteins.

In the present work, we have begun such a biophysical characterization of ER interactions by carrying out fluorescence-based binding assays on the interaction between full-length baculoviral expressed human ERα and its target DNA response element. Our equilibrium assays are based on the observations of changes in the fluorescence anisotropy of a fluorescein labeled target upon binding by the protein. Because rotational diffusion of the free oligonucleotide is quite rapid, the anisotropy of the fluorescent dye covalently bound to the oligonucleotide is quite low, i.e., little of the orientation of the polarized exciting light is retained in the emission. However, because binding by the protein significantly slows the rotational diffusion of the oligonucleotide, much more of the polarization of the excitation is retained in the emission. These measurements can be made with very low concentrations of DNA target and can provide data of very high precision and reproducibility. Thus, they can be used to characterize quantitatively the affinity, cooperativity and eventually the kinetics of biomolecular interactions. Earlier, we reported measurements on ER–ERE interactions, but the labeling scheme used in these prior studies did not yield data of the quality required to determine cooperativity and small differences in affinity (16). Here we expand upon this earlier work, testing the effects of salt, ligand, temperature and target sequence on the full-length human ERα–ERE interactions.

MATERIALS AND METHODS

Protein

Full-length purified baculovirus expressed ERα was purchased from Panvera corp (Madison, WI). The concentration of active receptor in each preparation was determined by the supplier by tritiated estradiol binding and compared to the concentration of total protein obtained by Bradford analysis. All preparations were over 80% pure and active. Thus the concentration of protein was taken to be the concentration of protein capable of binding estradiol, and not the total protein concentration. The protein was stored in aliquots of 50 µl at –80°C.

Oligonucleotides

Labeled oligonucleotides were purchased in HPLC purified form from Eurogentec (Seraing, Belgium) for the internally labeled target and from Genosys (Montigny-le-Bretonneux, France) and Genset (Paris, France) for the F-vitERE and mutant targets respectively. The fluorescein label was incorporated by the supplier using phosphoramidite chemistry, and all free probe was thus eliminated in the synthesizer and subsequent HPLC purification. The labeling ratio for the sense strand was calculated using known extinction coefficients for the four bases and the oligonucleotide composition and a molar extinction coefficient of 90 000 M^{-1} cm^{-1} for the fluorescein. All oligonucleotides presented labeling ratios between 40 and 80%. The sense and anti-sense strands were annealed by heating a 1.1 molar ratio of unlabeled anti-sense with labeled sense to 85°C for 10 min in 10 mM Tris buffer in the presence of 0.1 mM EDTA, 0.1 mM DTT, pH 7.5 (TD buffer) and cooling slowly to room temperature in a beaker with the heating water set on the bench. Annealed oligonucleotides were stored at –80°C.

Ligands

17-β-Estradiol (E2), 4-hydroxy-tamoxifen (OH-Tam) were purchased from Sigma Chemicals (St Louis, MO) and ICI 182780 (ICI) was a kind gift from Astra Zeneca (London). Ligands were stored at –20°C in ethanol at 1 mM or diluted into the TD buffer.

Anisotropy assays

Binding assays were performed using a Beacon 2000 polarization instrument regulated at the indicated temperature. Target oligonucleotide concentration was 1 nM. Each point in the titration curve was obtained by starting with 1 ml of a solution of 82 nM ER. Aliquots of 200 µl were successively removed from the starter solution and replaced by 200 µl of buffer solution containing 1 nM in DNA. The buffer solution was 10 mM Tris–HCl, 0.1 mM EDTA, 0.1 mM DTT, pH 7.5, and contained the indicated concentration of KCl. Tubes were equilibrated at the temperature of the measurement for 5 min prior to measurement and the anisotropy was measured successively until stabilized. The reported values are the average of three to five measurements after stabilization.

Data analysis

Binding data of all types were analyzed using the package BIOEQS, which differs somewhat from the approaches habitually used. The binding program used by our group, BIOEQS, was developed in 1991 (17–19) as a means for analyzing systems that may include a number of oligomeric protein species, in various states of ligation. In order to easily analyze data according to complex models and to test various models incorporating different sets of species, the program makes use of a numerical, rather than analytical, solver engine. Instead of deriving an analytical expression for the binding isotherm in terms of dissociation constants implicit in the model of choice, the simultaneous set of non-linear free energy equations associated with the model is solved numerically in terms of the concentrations of the individual species postulated to exist. The free energies that are recovered from the fits using this program correspond to the free energies of formation of each postulated species (i.e., dimer/DNA complex) from the free elements (free dimer and free DNA).

The model which was employed to fit the FC6-25mer profiles corresponds to the case of a system in which a protein binds to DNA in both a 1:1 and in a 2:1 monomer/DNA complex (see schematic below). The first free energy in the model, ΔG°_1, corresponds to the free energy of formation of the 1:1 monomer/DNA complex (MDNA) from free monomer (M) and free DNA, while the second free energy, ΔG°_2, corresponds to the free energy of formation of the 2:1 monomer/DNA complex (M_2ERE), also from free monomer and free DNA. In order to calculate the free energy of binding of the second monomer to the 1:1 dimer/DNA complex, ΔG°_{21}, ΔG°_1 must be subtracted from ΔG°_2. The cooperative free energy ΔG°_{coop}, is calculated as the difference between ΔG°_2 and two times ΔG°_1.

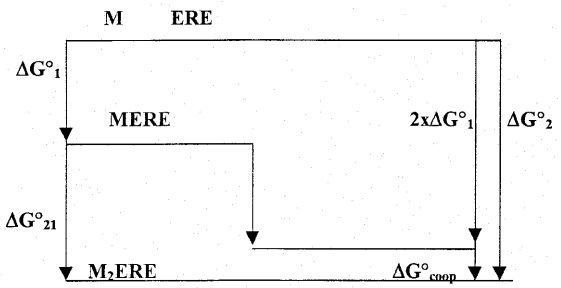

With each marquardt minimization iteration, the solver uses the current free energy values, along with the mass balance constraints (i.e., total protein and DNA concentrations) to calculate the species concentrations using an iterative constrained optimization routine with the mass balance constraints incorporated by Lagrange multipliers. The calculated data are generated from this numerically derived species concentration vector according to the user specified observable mapping scheme. In this way, the user must indicate how each individual species is related to the experimental observable. The plateau values for the anisotropies were floating parameters in the fits, while the anisotropy corresponding to the intermediate monomer-bound DNA species was fixed at a value approximately half-way between the two plateaus. The details of this program have been given elsewhere (17–19). Uncertainties on the recovered parameters were obtained by repeating a complete minimization over a range of tested parameter values, allowing all other parameters to float. The reported errors represent the uncertainties at the 67% confidence limit (i.e., 1 standard deviation) taking into account the correlation between all the parameters in the fits.

RESULTS AND DISCUSSION

In earlier collaborative work with the group of J. Gorski (16), we used a rhodamine labeled target oligonucleotide to study ER–ERE interactions. However, due to high probe mobility, and inefficient labeling, the quality of the anisotropy data obtained in those previous titrations did not permit us to determine whether the binding of ER to its target ERE was cooperative in nature. The present studies are designed to provide data of sufficient quality for establishing whether or not binding is cooperative and for comparison of binding affinities under a variety of conditions and for a variety of target sequences. In order to achieve the necessary precision in the data, we have used two different labeling schemes for the target oligonucleotides, either through a 5′-phosphoramidite-six carbon linkage on the sense strand of the target site, or alternatively, incorporated internal to the sequence in place of the thymine base at position +5 from the 5′-end of the sense strand. The fluorescent probe used was fluorescein to maximize the sensitivity of the assay. Both types of labeling yielded good quality data and binding constants within error of each other under similar conditions. The oligonucleotides were 35 bp in length and derived from the palindromic ERE upstream of the vitellogenin promoter. The wild-type target sequence referred to here as F-vitERE and has the sequence given below for the sense strand.

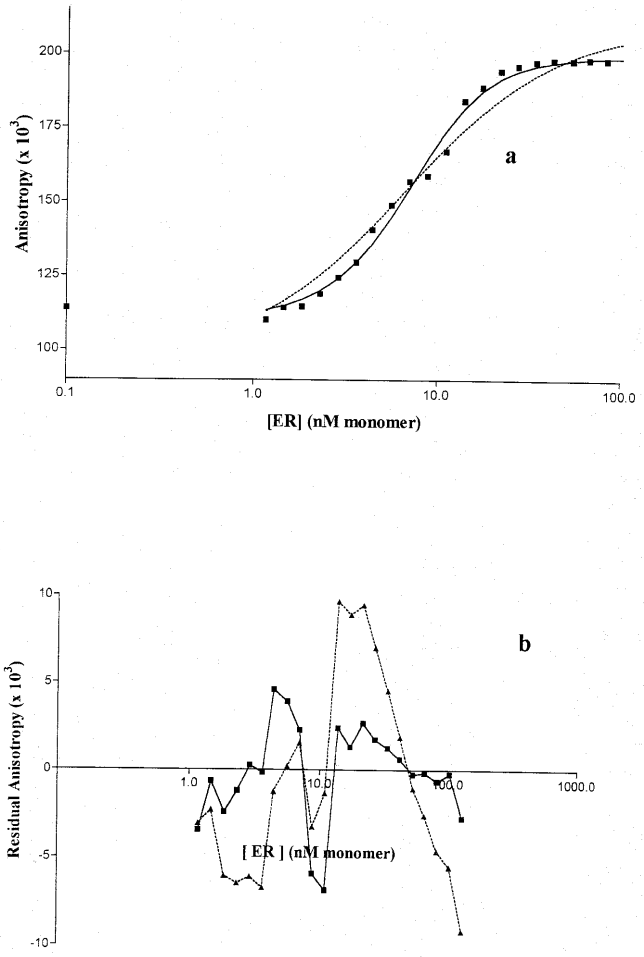

Figure 1. (**a**) Fluorescence anisotropy profile of full-length human ERα binding to 1 nM 5′-fluorescein labeled vit-ERE in 200 mM KCl in TD buffer at 21°C. The full line through the data points represents the fit to the data using the cooperative model including a monomer-bound intermediate as described in the Materials and Methods. The dotted line represents a fit with a simple binding model. (**b**) Residuals of the fit to the cooperative (full line) and simple (dashed line) binding models. The point plotted at the lowest protein concentration is in fact obtained in the absence of protein.

F-5′-AGCTTCGAGGAGGTCACAGTGACCTGGAGCGGATC-3′
F-vitERE

Figure 1a shows the anisotropy-based binding isotherm obtained upon titration of the 5′-fluorescein labeled wild-type ERE 5′-F-vitERE with purified full-length human ERα at 21°C in the presence of 200 mM KCl in the TD buffer. No changes in fluorescence intensity accompanied the increase in anisotropy, and lifetime measurements on the free and bound fluorescein labeled oligonucleotide revealed identical 4.3 ns decay for the free and bound species. The anisotropy increase obtained under these buffer conditions could be reversed by addition of unlabeled vit-ERE, but not by addition of poly(dI–dC) (data not shown), demonstrating the specific nature of the interaction. The solid line through the points represents a fit of the anisotropy data in Figure 1a to the model described in the

Materials and Methods. A total of seven binding profiles for the ER interaction with the F-vitERE target were analyzed. The average value over the seven data sets for the total free energy for the binding of two monomers ΔG°_2 to the ERE of –21.8 ± 0.9 kcal/mol and the average value of the ΔG°_{coop} is found to be 1.7 ± 0.7 kcal/mol. In terms of affinity, one can calculate an apparent C1/2 (concentration of 50% bound) from half of the value of ΔG°_2. This corresponds to an apparent K_d of 9 nM. There is a reasonably high degree of uncertainty on the value of the cooperativity since under highly cooperative conditions the value of ΔG°_1 is not well determined because the intermediate monomer-bound DNA species is never highly populated.

It can be seen quite clearly from Figure 1a and b that the cooperative model provides a much better fit to the data (compare full to dashed lines). This model, implicating an intermediate monomer-bound species, has been used to analyze the interaction of the estrogen receptor DNA binding domain (ER-DBD) with the ERE (14,15). However, in that case, such a model was clearly justified since the ER-DBD is monomeric in solution up to millimolar concentrations. In the case of the full-length ER used here, the concentration dependence of its oligomeric state has not been determined. We have found that the isolated hormone binding domain (HBD) of ER remains dimeric down to a concentration of 1 μM (unpublished results). We can suppose that the tendency to form dimers would be greater for the full-length receptor since both the HBD and DBD dimerization domains are present. The fact that the protein binds cooperatively to its target demonstrates that there is protein–protein interaction linked energetically to the protein–DNA interaction in this system. Although the final stoichiometry of the complex cannot be unambiguously deduced from the data in Figure 1a, it is highly likely that it corresponds to one dimer per target oligonucleotide. We base this assumption on what is known of the structure of the ER-DBD–ERE interaction (20) and the small size of the oligonucleotide. We note that the two possible mechanisms of the cooperativity (intermediate free dimer or intermediate bound monomer) are equally likely. Only stopped-flow kinetic measurements in the future will allow the determination of which of these two mechanisms is operative.

Salt effects on ER–ERE interactions

The effect on ER–ERE interactions of varying the concentration of KCl in the binding buffer at 21°C is shown in Figure 2a and b. As before (16) we find that decreasing the salt concentration yields profiles exhibiting a much larger increase in anisotropy, indicative of the formation of complexes of significantly higher stoichiometry. At 150 mM, for example, the total change is 40 mA units, whereas at 200 mM KCl the total change is only ~32 mA units. Between 200 and 300 mM KCl the effect of salt on the specific dimer–DNA interaction is quite large, consistent with the 12 phosphate contact observed in the crystal structure of the ER-DBD complexed with DNA (20,21). A similarly strong salt concentration effect has been observed for the GR-DBD/GRE interaction (22, J.J.Hill, C.A.Royer and K.R.Yamamoto, unpublished results). We note that the loss of cooperativity at higher salt concentration arises because the ER is likely to be in the form of a pre-formed dimer at the higher concentrations of protein required for binding in the presence of higher salt concentrations.

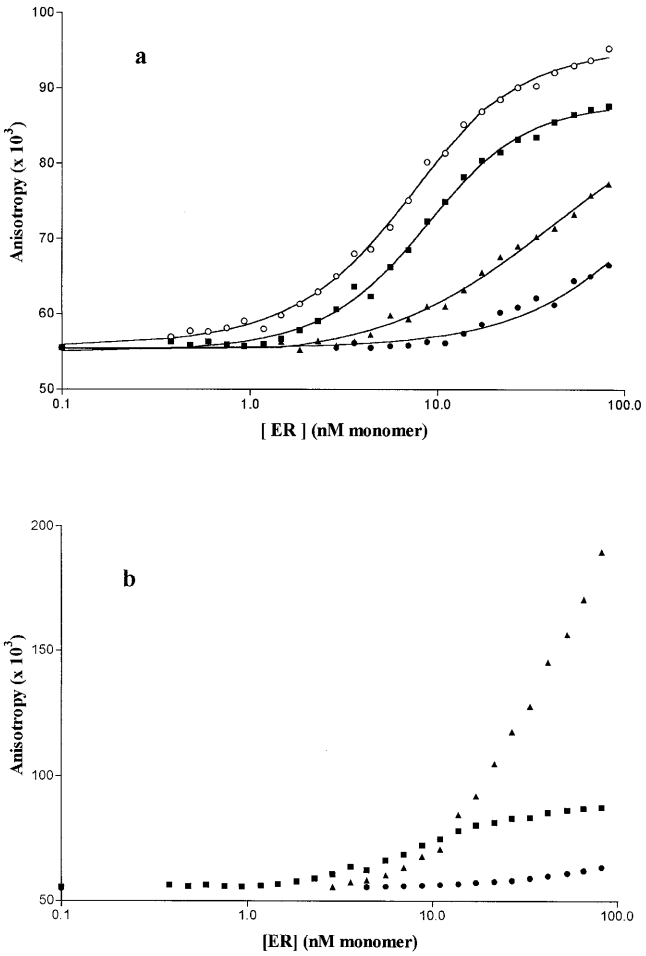

Figure 2. Salt concentration dependence of ER–ERE interactions. (**a**) Profiles for titrations of F-vitERE obtained in presence of 150 (open circles), 200 (squares), 250 (triangles) and 300 mM KCl (closed circles); (**b**) profiles obtained for F-vitERE at 200 mM KCl (squares), a mutant sequence mutF (see Fig. 5) at 200 mM KCl (circles) and in the absence of salt (triangles). The profiles were obtained in TD buffer at 21°C, and the DNA concentration was 1 nM. In this case the DNA target was labeled on the 5′-end through a six-carbon linker. Lines through the points represent fits to the data in terms of the model described in the Materials and Methods. The points plotted at the lowest protein concentration were obtained in the absence of protein.

In Figure 2b, a more striking example of the effect of lowering the salt concentration on the complex stoichiometry and also specificity can be seen. The nearly flat profile in circles corresponds to a titration at 200 mM in KCl of ER onto a mutant labeled oligonucleotide that exhibits much lower affinity for the protein than the wild-type sequence (see below). Squares correspond to ER binding to the wild-type F-vit-ERE in the presence of 200 mM KCl, and the triangles correspond to ER binding to the mutant sequence in the absence of added KCl to the TD buffer. This large increase in anisotropy in the absence of salt is quite similar to the previously reported binding of ER to a wild-type rhodamine labeled vit-ERE in the absence of salt (16), and data on GR-DBD–GRE interactions under the same conditions (J.J.Hill, C.A.Royer and

K.R.Yamamoto, unpublished results). The very large increase in anisotropy indicates formation of non-specific complexes of very high stoichiometry, but reasonably high apparent affinity since binding begins just above 10 nM in ER.

Effect of ligands on ER–ERE interactions

Although Gorski and co-workers (3,5,16) have reported previously that ER does not require ligation by estradiol (E2) for high affinity binding to its response element, others have reported that cooperative binding depends upon ligation (12), that tamoxifen liganded receptor releases partially its tamoxifen ligand upon binding to EREs (12) and that binding sensograms using SPR are highly ligand dependent (13). Such behavior would implicate energetic coupling between DNA binding, ligand binding and even protein–protein interactions. These observations of specific ligand effects on interaction with DNA may arise from the use of non-equilibrium assay techniques, unpurified receptor, *in vivo* assays and complex response elements. Besides our recently reported anisotropy assays (16), no *in vitro* studies had been carried out under true equilibrium conditions using purified receptor, and the quality of our recently reported data lacked somewhat in precision. Moreover, we did not test ER ligands other than estradiol (E2) in that study. In order to clarify whether or not ligands play a role in modulating ER–ERE interactions, we have carried out the equilibrium anisotropy-based titrations in the absence and presence of a variety of ER ligands.

Figure 3a and b shows the binding profiles of ER to the internally labeled fluorescent vit-ERE in the absence of ligands and in the presence of estradiol (E2) (Fig. 3a) or the partial agonist 4-hydroxytamoxifen (OH-Tam) or the antagonist (ICI) (Fig. 3b) at 200 mM KCl and 21°C in TD buffer. The results of the analysis of the data in Figure 3a and b can be found in Table 1. The reader may remark on a difference in apparent affinity between the profiles observed in absence of ligand in Figure 3a and b. This is due to slight differences in the DNA binding activity between each lot of receptor. We note that active receptor concentration is determined by the supplier using a radio-labeled E2 binding assay. However, we have noted these small differences between batches of ER and, therefore, when comparing the effects of various assay conditions we are careful to make these comparisons using the same batch. Regardless of the batch or the type of ligand used, the apparent affinity of ER for the ERE does not change significantly with ligand.

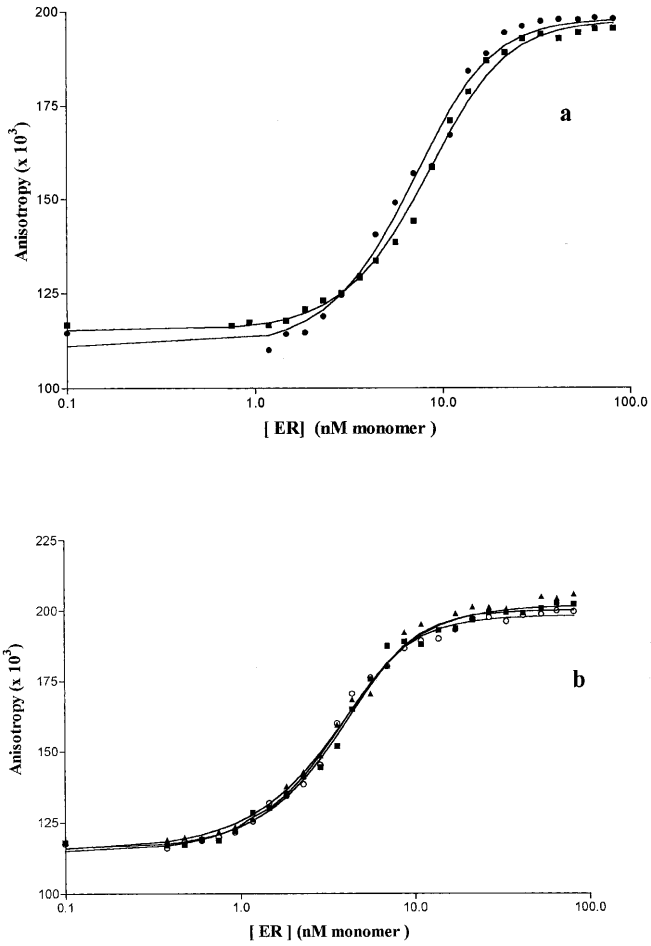

Figure 3. Ligand dependence ER–ERE interactions. (**a**) F-vitERE titrated with ERα in the absence of ligand (squares) and in the presence of 0.1 mM E2 (circles); (**b**) F-vitERE titrated with ERα in the absence of ligand (squares), in the presence of 0.1 mM ICI (triangles) and in the presence of 0.1 mM OH-Tam (circles). The profiles were obtained in TD buffer in the presence of 200 mM KCl at 21°C, and the DNA concentration was 1 nM. In this case the DNA target was labeled through a fluorescein labeled thymine residue at position +5 from the 5′-end. Lines through the points represent fits to the data in terms of the model described in the Materials and Methods. The points plotted at the lowest protein concentration were obtained in absence of protein.

Effect of temperature on ER–ERE interactions

The binding profiles for ER with F-vit-ERE at 4, 21 and 32°C are shown in Figure 4. Due to differences in anisotropy at the different temperatures arising from viscosity effects we have fit the raw data and then normalized both data and fit for comparison. It can be seen that there is no significant difference between these profiles. The values for the recovered free energies are given in Table 1. Because the differences are not significant we have not attempted to extract values for the enthalpy, entropy or heat capacity changes that may accompany this interaction. There could be a slight increase in apparent affinity between 4 and 21°C, but then the lack of further increase between 21 and 32°C could arise from non-linearity in the temperature dependence due to a heat capacity change or alternatively could be due to the onset of denaturation of the protein at this temperature. We note that full-length ER is quite fragile and we have had to take great care in the titrations to minimize mixing and heating in order to obtain reproducible results. In any case, the effects of temperature are very small, indicating that the enthalpy change upon binding is relatively small, and that the binding process is entropy driven. These results are consistent with a very in-depth study of Lundback and co-workers on the thermodynamics of the interactions between GR-DBD and a variety of mutants with target GREs (14,15).

Sequence determinants of ER–ERE interactions

Most natural EREs do not present the perfect palindromic repeat of the vitellogenin ERE. In order to assess the relative

Table 1. Free energy values for ER–ERE interactions

Temperature (°C)	[KCl] (mM)	Ligand 0.1 mM	ΔG°_1 (kcal/mol)	ΔG°_2 (kcal/mol)	ΔG°_{coop} (kcal/mol)
21 (Fig. 2)	200	–	10.6 ± 0.2	21.8 ± 0.1 (8.0×10^{-9} M)[a]	0.6
21 (Fig. 2)	250	–	10.4 ± 0.1	20.0 ± 0.1 (3.8×10^{-8} M)[a]	–0.6
21 (Fig. 2)	300	–	9.8+0.1/–0.4	18.7 ± 0.3 (1.4×10^{-7}M)[a]	–0.6
21 (Fig. 3a)	200	–	<8.6	21.9 ± 0.1 (7.4×10^{-9} M)[a]	>2.4
21 (Fig. 3a)	200	E2	<8.6	22.1± 0.1 (6.3×10^{-9} M)[a]	>2.4
21 (Fig. 3b)	200	–	<11.2	23.0 ± 0.1 (2.9×10^{-9} M)[a]	>0.6
21 (Fig. 3b)	200	OH-Tam	<11.3	23.1 ± 0.1 (2.7×10^{-9} M)[a]	>0.5
21 (Fig. 3b)	200	ICI	<11.8	23.1 ± 0.1 (2.7×10^{-9} M)[a]	>–0.5
21 (Fig. 4)	200	–	10.3 ± 1.0	23.0 ± 0.1 (2.9×10^{-9} M)[a]	2.4
4 (Fig. 4)	200	–	10.1 ± 0.2	21.50 ± 0.05 (3.3×10^{-9} M)[a]	1.3
32 (Fig. 4)	200	–	11.6 ± 0.2	23.9 ± 0.05 (2.7×10^{-9} M)[a]	0.65

[a]The values in parenthesis represent an apparent K_d value calculated from the value of the free energy for the binding of the two monomers divided by 2. This calculation was necessary because in most cases the binding was cooperative and a simple calculation of the K_d from the free energy of binding of the first monomer is not possible. This apparent K_d value gives the reader an idea of the concentration at which 50% binding occurs.

The concentration of the target oligonucleotides was between 1 and 2 nM. Conditions were otherwise as noted in the Materials and Methods. Uncertainties on the recovered free energy values were obtained by rigorous confidence limit testing, which involves refitting the curve at each tested value of the parameter. This method provides much more realistic (and larger) confidence limits than typically reported based on the diagonal of the correlation matrix. Moreover, with our method, the correlation between parameters is taken into account, whereas this is not the case otherwise.

contributions of each of the base pairs in the target site to the ER–ERE affinity we have made systematic symmetric purine→pyrimidine or pyrimidine→ purine substitutions by simply inverting the base pair between sense and anti-sense strands in both half sites for each of the six base pairs of the half site. The sequences of the mutated targets are given in Figure 5 and the binding profiles can be found in Figure 6. All of the mutants exhibited significantly lower affinities than the F-vitERE target, as can be seen by the large shift to higher protein concentrations of the binding profiles. We note that because of the prohibitive cost and limiting concentration of the ER we could not carry out the titrations above 100 nM in protein, and thus the binding profiles for the mutated sequences are far from complete. In order to obtain a semi-quantitative assessment of the relative affinities of the different targets, we have made the assumption that the value of the upper plateau of the anisotropy is the same as for the wild-type sequence. We have fit the profiles in terms of a simple binding model, since not enough data could be obtained to treat these profiles in terms of their eventual binding cooperativity. In order to compare the affinity for these sequences with that of the F-vitERE target, we have reported an apparent K_d for the wild-type target which is obtained using the value for half of ΔG°_2 (Table 2). This value can be thought of as an apparent C1/2 value.

Table 2. Effect of base pair mutations on ERα binding to the ERE target

Sequence	mutA	mutB	mutC	mutD	mutE	mutF	CathD
Fold loss K_{app}	25	42	36	34	81	31	17

Profiles were obtained using 1–2 nM fluorescein labeled target oligonucleotide in buffer, pH and 21°C. The K_{app} for the wild-type F-vitERE was calculated using $\exp[(\frac{1}{2}\Delta G^\circ_2)/RT]$, and the K_{app} for the mutant sequences was estimated as described in the text. The apparent K_d for the wild type was 8.0×10^{-9} M.

In Figure 6 we can distinguish clear differences between the raw data of the mutant target profiles, and these differences are likewise apparent in their apparent K_a values obtained from the fits (Table 2). The losses in affinity compared to the F-vitERE target range from 25-fold for the mutA target to 81-fold for the mutE target. The effect of the mutations can be best understood by referring to the schematic diagram (Fig. 7) of the contacts

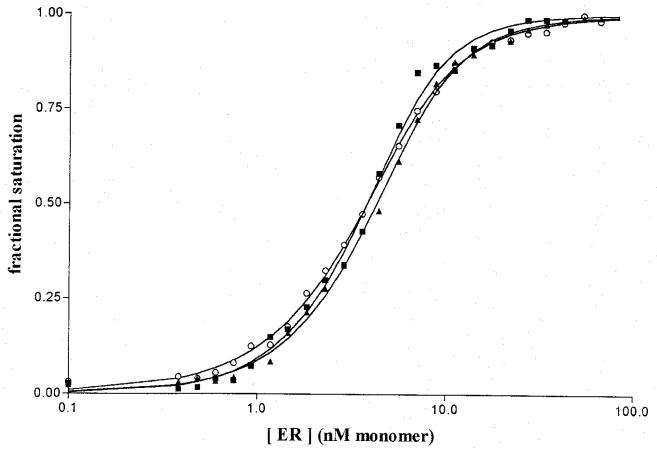

Figure 4. Temperature dependence of ER–ERE interactions. Normalized titrations for 4 (triangles), 21 (squares) and 32°C (circles). Profiles were obtained using the 5′-fluorescein labeled F-vitERE at a concentration of 1 nM in TD buffer with 200 mM KCl. The data were fit and then the raw data and the fits were normalized for comparison, to eliminate differences due to temperature dependence of solution viscosity. Lines represent fits of the data to the model described in the Materials and Methods. The points plotted at the lowest protein concentration were obtained in the absence of protein.

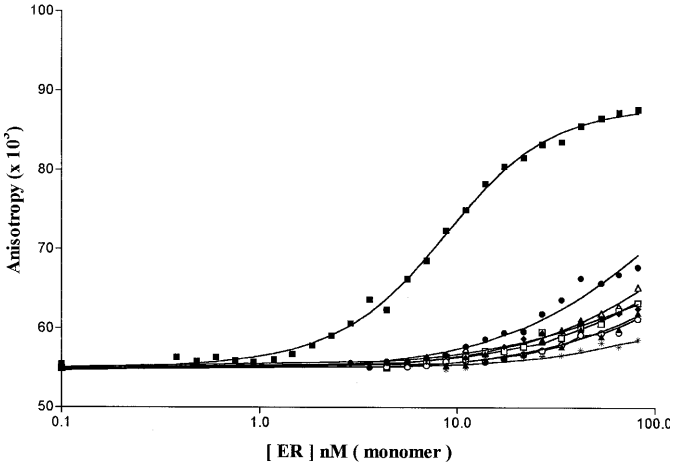

Figure 6. Sequence dependence of ER–ERE interactions. Titrations are shown for F-vitERE (closed squares), mutA (open triangles), mutB (open circles), mutC (closed triangles), mutD (diamonds), mutE (asterisks), mutF (open squares) and CathD (closed circles). Titrations were carried out using 1–2 nM target DNA in TD buffer at 21°C in the presence of 200 mM KCl. Lines through the points represent fits to the data for the mutant targets using a simple binding model, and for the F-vitERE using the cooperative model described in the Materials and Methods. The point plotted at the lowest protein concentration was obtained in the absence of protein.

F- ERE sense:

F-AGCTTCGAGGAGGTCACAGTGACCTGGAGCGGATC

F-ERE mutA sense

F-AGCTTCGAGGT GGTCACAGTGACCAGGAGCGGATC

F-ERE mutB sense

F-AGCTTCGAGGACGTCACAGTGACGTGGAGCGGATC

F-ERE mut C sense:

F-AGCTTCGAGGAGA TCACAGTGATCTGGAGCGGATC

F-EREe mutD sense:

F-AGCTTCGAGGAGGACACAGTGTCCTGGAGCGGATC

F-ERE mutE sense

F-AGCTTCGAGGAGGTGACAGTCACCTGGAGCGGATC

F-ERE mutF sense

F-AGCTTCGAGGAGGTCTCAGAGACCTGGAGCGGATC

F-Cath D sense

F-AG TTCGAGGGGGC CGGGCTGAC CCGGAGCGGATC

Figure 5. Sequences of the wild-type and mutant oligonucleotides used in the present study. These targets were all 5′-labeled with fluorescein through a six-carbon phosphoramidite linker as described in the text.

between the ER-DBD and its target ERE reproduced based on that given by Schwabe and co-workers (20) and based on their crystallographically determined structure. That mutations to the outermost base pairs of the half-site (mutA, 25-fold and mutF, 31-fold) result in the smallest perturbations to the affinity is understandable since no direct contacts to these bases are apparent in the crystal structure. Only phosphate contacts appear to extend to these bases. It is in fact somewhat surprising that the observed effect is so large, corresponding to ~1 kcal/mol per half-site. It is also surprising that the TA→AT mutation of the outermost of the central base pairs of the half-site (mutD), which is one of the two base pairs that determines the ER–GR specificity (22), resulted in only a 34-fold loss in apparent affinity, even though the thymine at that position appears to make contact with lysine 32 of ER-DBD (20). However, since this residue makes a number of other contacts with the target, there may be some compensatory mechanism. Mutation (GC→CG, mutC) of the other central base pair that determines the GR–ER specificity results in only a slightly larger loss in affinity (41-fold), even though lysine 32 and glutamate 25 make a number of direct and water-mediated contacts to the 06 and N7 of the guanine, and the N4 of the cytosine. In fact, the loss in affinity upon mutation of the second base pair in the half site (mutB, GC→CG) perturbs the interaction to the same extent (42-fold). In this case, lysine 28 makes a contact to the O6 of the guanine. The largest perturbation is found for the CG→GC mutation (mutE) of base pair at position 5 of the 1-AGGTCA-6 half site. At this position arginine 33 of the ER-DBD appears to make contacts with both the N7 and the O6 of the guanine, although the contact to the O6 appears to be a water-mediated bifurcated contact involving

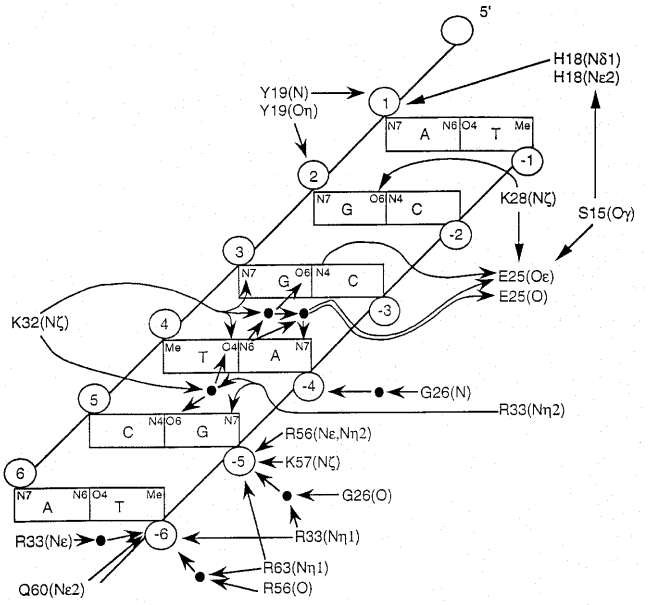

Figure 7. Schematic representation of the interactions between the ER-DBD and the target ERE reproduced from the schematic given by Schwabe and co-workers (20) based on their crystallographically determined structure. In our schematic the half site bases are labeled from 1 to 6 (sense strand) and –1 to –6 (anti-sense strand). Water molecules are represented by filled circles and H-bonds by arrows.

the O4 of the neighboring thymine. It is perhaps due to this complex network of interactions that mutation at this position leads to such a significant loss in affinity. Interestingly, the target oligonucleotide derived from the sequence of the cathepsin D ERE (Fig. 5) which exhibits a much larger number of mutations, particularly in the 5′-half site, yields a significantly higher affinity than any of the symmetrically mutated targets. The cathepsin D sequence is only 17-fold less effective than the F-vitERE target. However, comparing the mutations in the cathepsin D target (with respect to the vitellogenin-based ERE) we see that three of the mutations are at the least important positions (1 and 6) and moreover are A→G (purine→purine) rather than purine→pyrimidine mutations. Two of the mutations occur in the central three base pairs between half-sites and the T→ C mutation at position 4 of the 5′ half site maintains at least the N7 water-mediated contact with glutamate 25.

CONCLUSIONS

We have determined the affinity of the specific interaction of baculovirally expressed human ERα for its target ERE under a variety of conditions. First of all, the binding is clearly cooperative. Assuming that the final stoichiometry of the specific complex is two monomers per target ERE, this implies that the full-length ER dimer dissociates into monomers upon dilution in the nanomolar concentration range. The observed cooperativity of binding definitively rules out simple monomer interaction of ER with its target and implicates a protein–protein interaction coupled energetically to DNA binding. We have found a very strong effect of salt concentration on the affinity and the specificity of ER–ERE interactions. This observation is important, not simply from a structural point of view, but also to underline the importance of comparing the results of studies carried out under similar conditions. We find that below 200 mM in KCl, we begin to see the appearance of higher order non-specific complexes. At very low salt the ER exhibits very little, if any, specificity and very high stoichiometry. Between 200 and 300 mM KCl, the salt concentration dependence of the overall affinity is fairly consistent with the number of phosphate contacts observed in the crystallographically determined structure of the complex between the ER-DBD and its palindromic target (20). The temperature studies revealed almost no effect of changing temperature on the ER–ERE affinity. Of course in the absence of any large effect we cannot hope to analyze the interactions for the thermodynamic parameters associated with the binding, but these studies do indicate that the enthalpy of interaction must be rather small, and thus that the binding is entropy driven. This is consistent with studies of the GR-DBD–GRE interactions reported earlier (14,15). We also demonstrate unambiguously the lack of any effect of ligand binding (agonist or antagonist) on the equilibrium binding affinity between the ER and its DNA target at 21°C in 200 mM salt.

Finally, our exploration of the contribution of each of the base pairs in the palindromic ERE target demonstrates that each base pair contributes significantly to the overall affinity, although the ER/GR specificity arises from the identity of the central two base pairs of the half site. In their analysis of their crystallographically determined structure, Schwabe and co-workers (20) conclude that the discrimination of half-site sequence is not simply a matter of slotting a different discriminatory amino acid into a common framework, but also involves considerable rearrangement of side-chains to compensate for changes in local DNA structure. The energetic data provided here support the idea of a globally determined half-site, in which the energetic contributions to the overall structure and affinity are rather evenly distributed throughout the site.

ACKNOWLEDEGMENTS

The authors thank Dr Vincent Cavaillès for helpful suggestions. This work was supported by the CNRS, INSERM, La Fondation pour la Recherche Médicale, L'Association pour la Recherche sur le Cancer and the Région Languedoc-Roussillon. N.P. is a post-doctoral fellow (INSERM poste d'acceuil recherche clinique) and Emmanuel Margeat is supported by a doctoral grant from the French Ministère de l'Education, de la Recherche et de la Technologie.

REFERENCES

1. Mangelsdorf,D., Thummel,C. and Beato,M. (1995) *Cell*, **83**, 835–839.
2. McKenna,N.J., Lanz,R.B. and O'Malley,B.W. (1999) *Endocrin. Rev.*, **20**, 321–344.
3. Murdoch,F.E., Meier,D.A., Furlow,J.D., Grunwald,K.A.A. and Gorski,J. (1990) *Biochemistry*, **29**, 8377–8385.
4. Murdoch,F.E., Grunwald,K.A.A. and Gorski,J. (1991) *Biochemistry*, **30**, 10838–10844.
5. Furlow,J.D., Murdoch,F.E. and Gorski,J. (1993) *J. Biol. Chem.*, **268**, 12519–12525.

6. Murdoch,F.E., Byrne,L.M., Ariazi,E.A., Furlow,J.D., Meier,D.A. and Gorski,J. (1995) *Biochemistry*, **34**, 9144–9150.
7. Anderson,I., Bartley,C.R., Lerch,R.A., Gray,W.G.N., Friesen,P.D. and Gorski,J. (1998) *Biochemistry*, **37**, 17287–17298.
8. Klinge,C.M., Peale,F.V.,Jr, Hilf,R., Bambara,R.A. and Zain,S. (1992) *Cancer Res.*, **52**, 1073–1081.
9. Nardulli,A.M., Greene,G.L. and Shapiro,D.J. (1993) *Mol. Endocrinol.*, **7**, 331–340.
10. Obourne,J.D., Koszewsi,N.J. and Notides,A.C. (1993) *Biochemistry*, **32**, 6229–6236.
11. Anolik,J.H., Klinge,C.M., Hilf,R. and Bambara,R.A. (1995) *Biochemistry*, **34**, 2511–2520.
12. Kuntz,M.A. and Shapiro,D.J. (1997) *J. Biol. Chem.*, **272**, 27949–27956.
13. Cheskis,B.J., Karathanasis,S. and Lyttle,C.R. (1997) *J. Biol. Chem.*, **272**, 11384–11391.
14. Lundback,T., Cairns,C., Gustafsson,J.-A., Carlstedt-Duke,J. and Hard,T. (1993) *Biochemistry*, **32**, 5074–5082.
15. Lundback,T., Zilliacus,J., Gustafsson,J.-A., Carlstedt-Duke,J. and Hard,T. (1994) *Biochemistry*, **33**, 5955–5965.
16. Ozers,M.S., Hill,J.J., Ervin,K., Wood,J.R., Nardulli,A.M., Royer,C.A. and Gorski,J. (1997) *J. Biol. Chem.*, **272**, 30405–30411.
17. Royer,C.A., Smith,W.R. and Beechem,J.M. (1991) *Anal. Biochem.*, **192**, 287–294.
18. Royer,C.A. and Beechem,J.M. (1992) *Methods Enzymol.*, **210**, 481–505.
19. Royer,C.A. (1993) *Anal. Biochem.*, **210**, 91–97.
20. Schwabe,J.W.R., Chapman,L., Finch,J.T. and Rhodes,D. (1993) *Cell*, **75**, 567–578.
21. Record,M.T.,Jr, de Haseth,P.L. and Lohman,T.M. (1977) *Biochemistry*, **16**, 4791–4796.
22. Lefstin,J.A., Thomas,J.R. and Yamamoto,K.R. (1994) *Genes Dev.*, **8**, 2842–2856.